Journal of The Electrochemical Society, **158** (1) K6-K10 (2011)
0013-4651/2010/158(1)/K6/5/$28.00 © The Electrochemical Society

Photoresponsive and Ultraviolet to Visible-Light Range Photocatalytic Properties of ZnO:Sb Nanowires

Jyh Ming Wu,[a,z] Chiung-Wan Fang,[b] Lin-Tsang Lee,[b] Hsin-Hsien Yeh,[c,d] Yu-Hung Lin,[d] Ping-Hung Yeh,[e] Ling-Na Tsai,[c] and Li-Jiaun Lin[c]

[a]*Department of Materials Science and Engineering, Feng Chia University, Taichung 40724, Taiwan*
[b]*Department of Applied Mathematics, National Chung Hsing University, Taichung 402, Taiwan*
[c]*Material and Chemical Research Laboratories, Industrial Technology Research Institute, Hsinchu 310, Taiwan*
[d]*Department of Materials Science and Engineering, National Tsing Hua University, Hsinchu 300, Taiwan*
[e]*Department of Physics, Tamkang University, Tansui 251, Taiwan*

Zinc oxide (ZnO) doped antimony (Sb) nanowires have been synthesized for improving ultraviolet sensing and photocatalytic properties. Upon illumination by UV light (365 nm, 2.33 mW cm^{-2}), the photoelectric current of the ZnO:Sb nanowires exhibited a rapid photoresponse as compared to that of the ZnO nanowires. A highest ratio of photocurrent to dark current of around 48.8-fold was achieved in the as-synthesized ZnO:Sb nanowires. A UV-visible spectrophotometer was used to investigate the absorbance spectrum of the ZnO:Sb nanowires, which exhibited a high absorbance ratio with redshift effect in contrast to that of the ZnO nanowires. Visible-light photocatalysis and UV photoresponsive properties of the ZnO:Sb nanowires are superior to those of the ZnO nanowires.
 [DOI: 10.1149/1.3514618]

Manuscript submitted April 29, 2010; revised manuscript received October 13, 2010. Published November 24, 2010.

Zinc oxide (ZnO) nanostructures have been considered promising materials for electronic and photonic applications due to their large excitation binding energy of 60 meV with wide direct bandgap at 3.37 eV.[1] ZnO nanostructures have been doped with appropriate amounts of dopant (i.e., Bi, Al, In, and Sn),[2-4] which can modulate the electrical properties[5,6] for use as alternative transparent conducting oxides. For optoelectronic device applications, n-type ZnO nanowires have been widely investigated using ZnO doped by dopant impurity as mentioned above. However, the p-type ZnO nanostructures have rarely been investigated in comparison with n-type ZnO. To seek better p-type dopants, recently many authors have reported that ZnO doped by single acceptor, such as N,[7] P,[8] As,[9] and Sb,[10] exhibits superior electrical properties. Although the ZnO:N nanostructures are able to produce the p-type semiconductor properties, reliability is still a problem. Among the group V elements, the element of arsenic has much larger ionic radius than the oxygen atom and can produce the p-type ZnO:As. Antimony is inexpensive and has a ionic radius similar to Zn ion. Therefore, ZnO:Sb is an attractive material for the fabrication of p-type semiconductors. ZnO not only possesses superior applications in the optoelectronic field but is also a promising material for photocatalytic applications. In addition, ZnO doped with transition metal ions can enhance the activities of the photocatalyst because doping offers a way to trap and extend the lifetime of charge carriers.[11] Although ZnO nanostructures have been widely reported in the applications of gas sensor, solar cell, and optical devices,[12-14] visible-light photocatalytic and photoresponsive properties of the ZnO:Sb nanowires have rarely been investigated.

In this work, the Sb dopant is incorporated into ZnO nanowires using vapor transfer process to investigate the ultraviolet sensing and photocatalytic properties. As-synthesized ZnO:Sb nanowires possess high concentrations of oxygen vacancies with high absorbance ratio from UV to visible-light range (>200 nm) as compared to undoped ZnO nanowires. In addition, a high absorbance ratio of ZnO:Sb nanowires provides a superior photocatalyst to ZnO nanowires from UV to visible-light range. A UV sensing mechanism with photocatalytic activities of ZnO:Sb nanowires was investigated.

Experimental

The source materials of Zn (0.3 g, purity 99%, 200 mesh) and Sb (0.01, purity 99%, 200 mesh) powders were mixed in a specified Sb/Zn wt % ratio of 1:30. As-prepared source materials were loaded into an alumina boat and then placed in the center zone of quartz reactor (tube). In the beginning, an argon (Ar, purity 99.99%) flow rate of 80 sccm was introduced into the reaction system to maintain the vacuum pressure at 10 Torr at all times. After that, 1.0 sccm of oxygen flow (O_2, purity 99.99%) was introduced to the system while the temperature reached 600°C. This temperature was maintained for 30 min. Then the furnace was turned off and the quartz tube was cooled to room temperature under an argon flow. An alumina substrate 1 cm × 1 cm in length was placed around 2 cm downstream from the source material.

As-synthesized products of undoped ZnO (reference sample) and ZnO:Sb nanowires were characterized using field emission scanning electron microscopy (FESEM, HITACHI, S-4800), thin film X-ray diffraction (Bruker), and high resolution transmission emission microscopy (HRTEM, JEOL, JEM-3000F). The chemical analysis of the ZnO:Sb nanowires was conducted by high resolution X-ray photoelectron spectrometer (XPS, ULVAC-PHI, AES-650). FESEM equipped with cathodoluminescence (CL) was used to analyze the luminescent properties of the ZnO and ZnO:Sb nanowires by applying an accelerating voltage of 1.5 kV. Ultraviolet-visible spectrophotometry was performed (UV/vis, Hitachi U-3900 double-beam spectrophotometer) to determine the photocatalytic activities of the as-synthesized products. To investigate the photoresponsive properties, after the nanowires were grown on an alumina substrate, the Ag wires were bonded to the surface of the as-prepared devices using silver glue to serve as metal electrodes. The space between two electrodes is 2 mm. After the silver wires were bonded on the surface of the sample, the sample was heated to 120°C for 30 min in ambient air to initiate the solidification of the silver glue.

Results and Discussion

Figures 1a and 1b show the FESEM images of Sb doped and undoped ZnO nanowires, respectively. As-synthesized ZnO:Sb nanowires exhibited a high aspect ratio as compared with the ZnO nanowires. The ZnO:Sb and ZnO nanowire lengths ranged from a few hundreds of micrometers to thousands of micrometers. The diameters were approximately 80–150 nm for ZnO:Sb nanowires and 90–200 nm for ZnO nanowires. The X-ray diffraction (XRD) pattern of the as-synthesized nanowires exhibited a single phase of ZnO wurtzite structure, as shown in Fig. 1c. The Sb doping did not induce a second phase in the ZnO:Sb nanowires. HRTEM images in the inset image of Fig. 2a show that the ZnO:Sb nanowires grew along the [0001] axis, corresponding to a certain lattice spacing of ~0.52 nm.[2] X-ray photoelectron spectra (XPS) spectra in Fig. 2b

[z] E-mail: jmwu@fcu.edu.tw

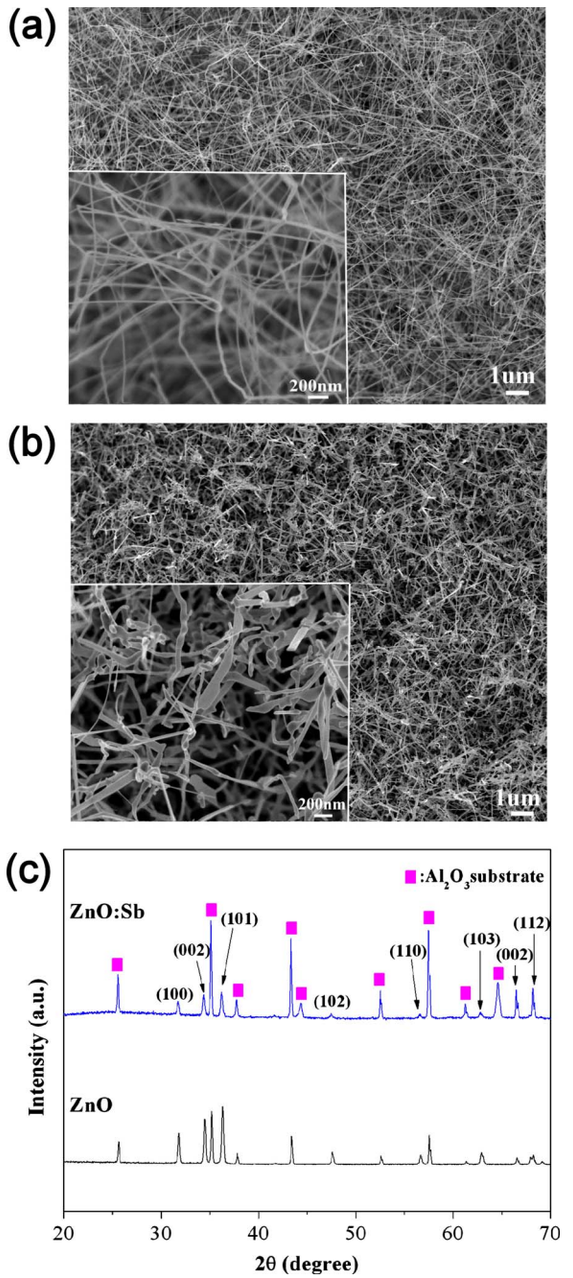

Figure 1. (Color online) (a) ZnO:Sb nanowires, the high-magnification SEM image is inset. (b) ZnO nanowires, the high-magnification SEM image is inset. (c) The XRD patterns of the as-synthesized Sb doped and undoped ZnO nanowires.

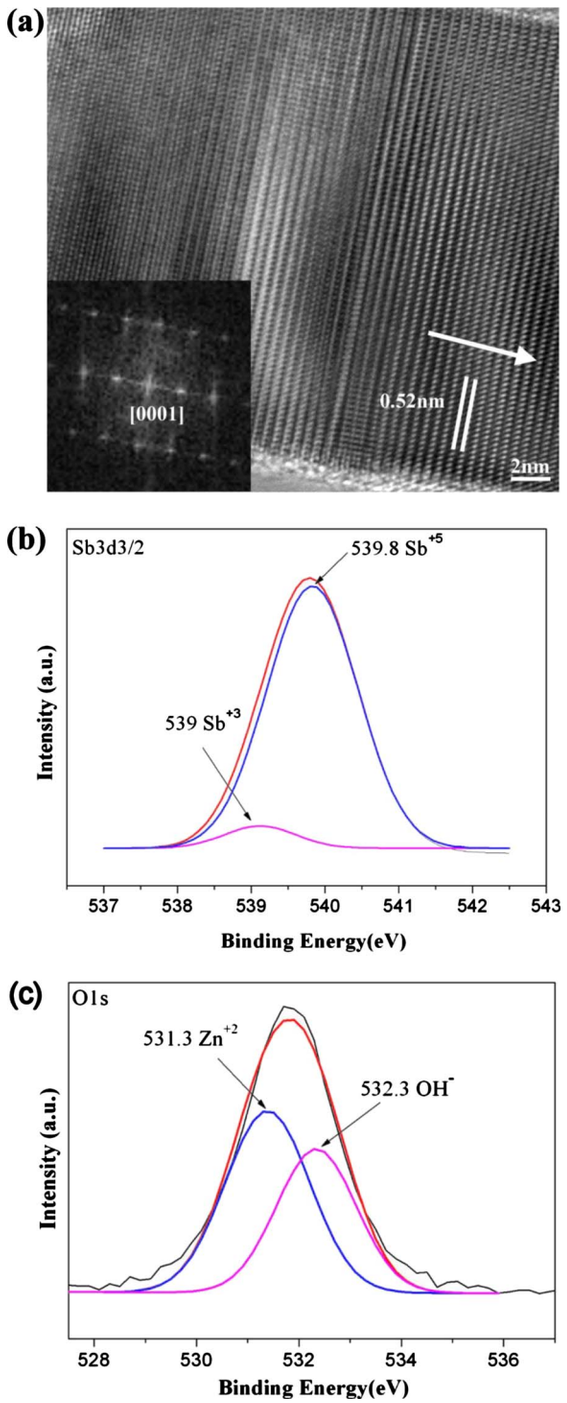

Figure 2. (Color online) (a) HRTEM image of ZnO:Sb nanowires, the corresponding SAD (converted by fast Fourier transform) pattern is inset. (b) Sb 3d3/2 core-level spectrum of ZnO:Sb. (c) O 1s core-level spectrum of ZnO:Sb.

show that the as-synthesized ZnO:Sb nanowires possess an additional peak at 539.8 eV, indicating that Sb^{5+} and Sb^{3+} were incorporated into the ZnO lattices. The O1s spectrum of Fig. 2c further demonstrated that the ZnO:Sb nanowires were concluded OH species. When antimony (Sb) was substituted for Zn instead of oxygen, two corresponding Zn vacancies were produced, which was an $Sb_{zn}–2V_{zn}$ compound[15] and formed a p-type semiconductor of ZnO:Sb. There is difficulty in using Hall measurement to investigate the behaviors of ZnO:Sb semiconductor nanowires as the nanowire morphologies differ from those of the thin film or bulk materials. Further investigation should be conducted by using the electrical measurement of single nanowire nanodevice to identify the semiconductor behavior of the ZnO:Sb nanowires.

The luminescent properties of ZnO:Sb nanowires and reference sample of undoped ZnO nanowires were investigated by CL. The CL spectra of ZnO:Sb nanowires showed that a very sharp intense blue emission peak occurred at 378 nm in contrast to that of the ZnO nanowires which occurred at 375 nm, as shown in Fig. 3. The ZnO:Sb nanowires exhibited a slight redshift in contrast to the ZnO nanowires. Both ZnO and ZnO:Sb nanowires possessed oxygen vacancies at around 450–550 nm. However, the Sb doping induced a

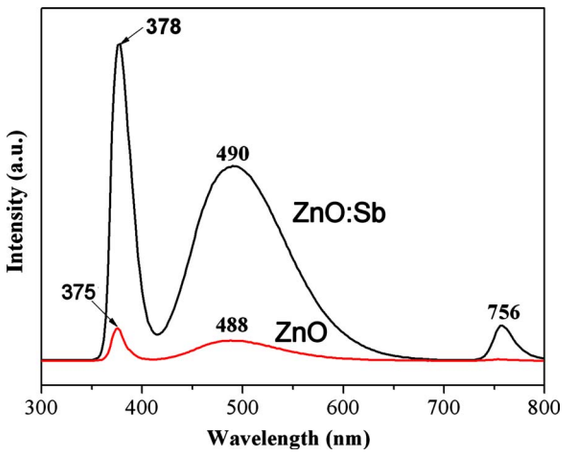

Figure 3. (Color online) The CL spectra of the ZnO:Sb and ZnO nanowires.

strong green emission. This is due to doping with cations which tend to induce the formation of oxygen vacancies in sites where there is a competition between Zn and Sb atoms during crystal growth.[16,17]

As-prepared ZnO and ZnO:Sb nanowires were grown on alumina substrates with the same area to investigate their photocatalytic activities. The absorbance ratios are shown in Fig. 4a. The absorbance ratio of ZnO:Sb was significantly higher than that of the ZnO nanowires, not only in the UV light region but also in the visible-light region ($>$400 nm), and a redshift effect was observed for ZnO:Sb nanowires. The CL and absorbance spectra demonstrated that a redshift effect occurred in the ZnO:Sb nanowires. The redshift is ascribed to the fact that Sb doping can narrow the bandgap of ZnO and implies that intraband transitions have been formed in the as-synthesized ZnO:Sb nanowires.

The photocatalytic activities were investigated by immersing the samples into methylene blue (MB, $C_{16}H_{18}ClN_3S{\cdot}H_2O$, 10 μM) solution. As-synthesized nanowires were irradiated under UV ($\sim$254 nm) and visible-light ($>$400 nm) for 0, 60, 90, and 120 min during which the change in the concentration of MB was monitored. Under exposure to UV and visible light, photodegradation ratios of the MB solution with and without nanowires versus exposure time are shown in Figs. 4b and 4c, respectively. The MB solution without nanowires exhibited a low photodegradation ratio during UV and visible-light irradiation. Figure 4b shows that the photocatalytic activities of the ZnO:Sb nanowires were superior to those of the ZnO nanowires after 60 min of exposure to UV irradiation. As expected, Fig. 4c further shows that the degradation ratio of the ZnO:Sb nanowires exhibited superior photocatalytic activities to those of the undoped ZnO nanowires after 1 h of visible-light irradiation. This may due to the higher absorbance ratio of the ZnO:Sb nanowires in comparison to undoped ZnO nanowires under visible-light irradiation. The high absorbance ratio of ZnO:Sb in the UV range resulted in higher electron–hole pair generated ratio of ZnO:Sb nanowires when compared with ZnO nanowires. In addition, doping with Sb^{5+} (and Sb^{3+}) resulted in a redshift effect, which can be attributed to the charge-transfer transitions between Sb^{5+} (and Sb^{3+}) electrons and the ZnO conduction band.[4] The presence of electron occupied intraband gap levels in ZnO:Sb photocatalysts may be responsible for the visible-light absorption.[18] A decreasing bandgap (or introduction of intraband gap states) results in more visible-light absorption.[19] Therefore, the photocatalytic activities of ZnO:Sb nanowires are superior to those of the ZnO nanowires from UV to visible-light range.

As-synthesized nanowires were fabricated into a nanosensor device to evaluate the UV sensing properties. The silver (Ag) electrode was bonded on an as-prepared sample as shown in Fig. 5a. The devices were placed under a dark box with a UV lamp (λ = 365 nm, intensity = 2.33 mW cm^{-2}). Figure 5b shows the applied

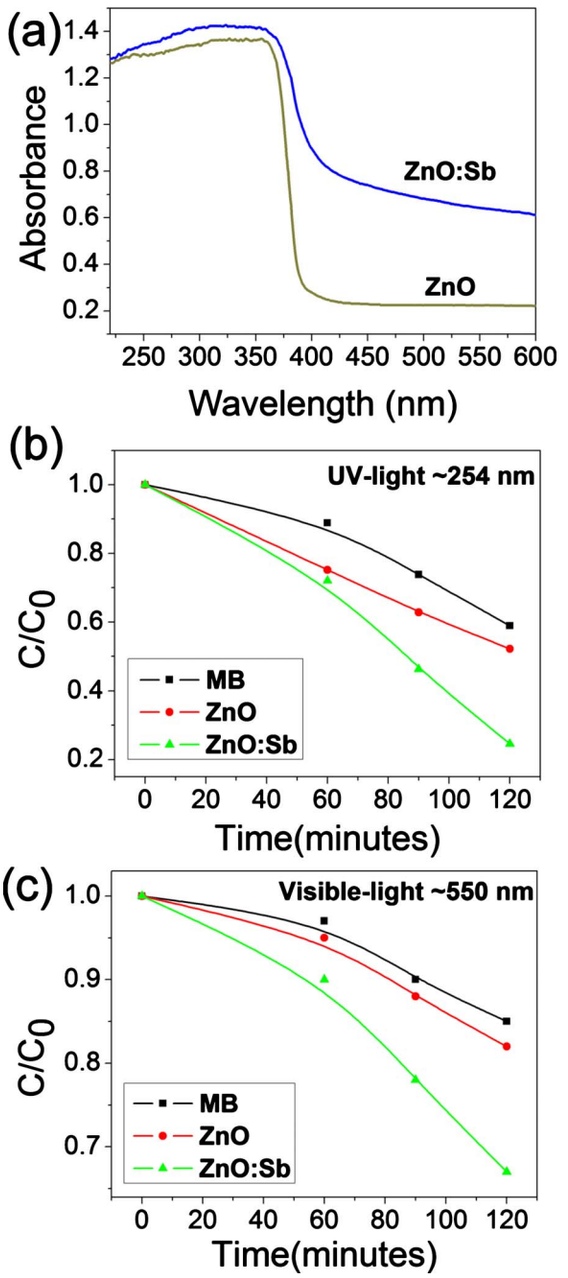

Figure 4. (Color online) (a) The absorbance spectra of the ZnO:Sb and ZnO nanowires. (b) UV light of photodegradation ratio (C/C_0) and (c) visible-light of photodegradation ratio (C/C_0) of MB solution using synthetic ZnO:Sb and ZnO nanowires and reference sample.

voltage from −5 to + 5 V bias as a function of device current. It is clear that the current–voltage (I–V) curves are almost linear, indicating that ohmic contacts were formed between the nanowires film and electrode.[20] The conductance of ZnO:Sb nanowires was lower than that of the ZnO nanowires. The UV on/off ratio was defined as I_{UV}/I_{Dark}, where I_{UV} is the photocurrent of the sensor (UV lamp in the on-state) and I_{Dark} is the dark current of the sensor (UV lamp in the off-state). The on/off ratio for the ZnO:Sb and ZnO nanowires were around 4880 and 156%, respectively. The response (t_{res}) and recovery times (t_{rec}) of sensor devices are shown in Fig. 5c. The response and recovery times were defined as the times required to reach 90% of the maximum and minimum final equilibrium values

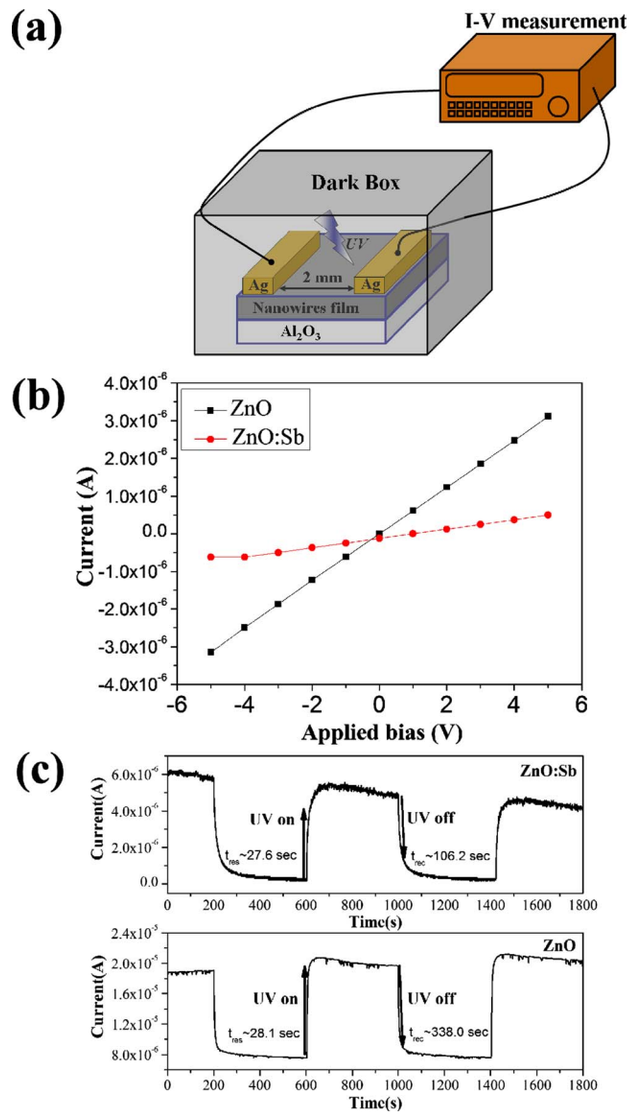

Figure 5. (Color online) (a) Schematic diagram of UV photodetector. (b) Dark *I–V* characteristic of the UV photodetector. (c) Photoresponse as a function of time with UV lamp in on and off states.

from the base value, respectively.[21] For the ZnO:Sb and ZnO nanowires, the response times were estimated to be 27.6 and 28.1 s, respectively. The recovery time of ZnO:Sb was estimated to be 106.2 s, while that of ZnO was estimated to be ~338.0 s. Under steady state, the photocurrent decreased as time increased. This is ascribed to the oxygen defect site combining with the hydroxyl group, which is gradually replaced by stronger oxygen bonding as described by Ahn et al.[22]

As mentioned above, Sb substitutes for Zn atoms, producing two corresponding Zn vacancies (Sb_{zn}–$2V_{zn}$) and forming a p-type semiconductor of ZnO:Sb. A nonstoichiometric metal deficiency ($M_{1-\delta}O$) is therefore formed in the ZnO:Sb compound as shown in reaction 1. However, in this work the CL spectrum revealed a very high intensity of oxygen vacancies in the green emission band. Oxygen deficiency ($MO_{1-\delta}$) can occur at oxygen sites because there is competition between Zn and Sb, as expressed in reaction 2. From the characteristics of UV photoresponse and CL spectrum, we suggest that the oxygen deficiency in reaction 2 dominates in the as-synthesized ZnO:Sb nanowires, as shown by the investigation of defect chemistry below

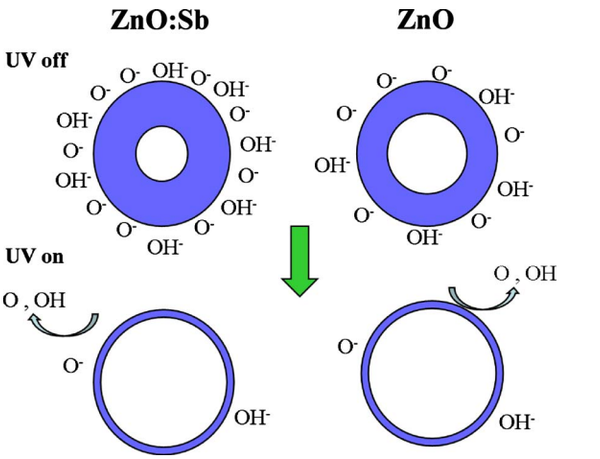

Figure 6. (Color online) Illustration of the gas adsorbed/deabsorbed status of the cross-sectional ZnO:Sb and ZnO nanowires between UV on and off states.

$$1/2O_2 \rightarrow O_o + V''_{Zn} + 2h^{\cdot} \quad [1]$$

$$O_o \rightarrow V^{\cdot\cdot}_o + 1/2O_2 + 2e' \quad [2]$$

$V^{\cdot\cdot}_o$ represents two positively charged vacancies (relative to a perfect lattice) on an oxygen site.

In terms of the UV sensing properties, the high concentration of oxygen vacancies induced a high intense green emission in ZnO:Sb nanowires when compared with ZnO nanowires (see CL image in Fig. 3 above). Accordingly, the oxygen vacancies of ZnO:Sb nanowires might combine with the oxygen and hydroxyl groups on the surface of the nanowires. The schematic diagram of the cross-sectional nanowire is shown in Fig. 6. As UV lamp is in the off-state, the depletion zone of the ZnO:Sb nanowires was thicker than that of the ZnO nanowires. This is attributed to the high concentration of oxygen vacancies, which induced electron carriers in the ZnO:Sb nanowires to maintain the charge neutrality. These electrons charged the O and OH groups to form the ion states of O^- and OH^- on the surface of ZnO:Sb nanowires, resulting in a thick depletion zone in ZnO:Sb in contrast to undoped ZnO nanowires. In addition, the absorbance ratio of the ZnO:Sb nanowires was higher than that of the ZnO nanowires in UV range (i.e., 200–400 nm). High concentration of photogenerated electron–hole pairs in ZnO:Sb nanowires means that there are higher concentrations of charged ion state, O^- and OH^-, on the surface of ZnO:Sb nanowires than on the surface of ZnO nanowires. By switching the UV lamp to on-state, the energy of the incoming UV photons was used to generate electron–hole pair separations. The holes might be recombined with the oxygen and hydroxyl groups (O^- and OH^-) to release the oxygen and hydroxyl in gas, and consequently, the free carriers can be infused into the conduction band of the as-synthesized nanowires, making a thinner depletion zone, as shown in the bottom section of Fig. 6. Here, we should note that both the depletion zones from the ZnO:Sb and ZnO nanowires recovered to their initial states under the same intensity of UV irradiation. The ZnO:Sb nanowires adsorbed more species of O^- and OH^- on their surface in contrast to the ZnO nanowires during the UV off-state. As UV was switched to on-state, a higher number of these charged ions released the carriers and then infused to the conduction band in the ZnO:Sb nanowires than those in the ZnO nanowires. The UV on/off ratio of the ZnO:Sb nanowires was higher than that of the ZnO nanowires.

Conclusion

The ZnO:Sb and ZnO nanowires were synthesized on alumina substrates by a vapor–solid process. In the CL and absorbance spectra, a redshift effect occurred for the as-synthesized ZnO:Sb nano-

wires in contrast to the ZnO nanowires. CL spectrum of ZnO:Sb nanowires showed a high intensity of oxygen vacancies at around 490–550 nm. The UV on/off ratio of ZnO:Sb nanowires was superior to that of the ZnO nanowires based on defect chemistry investigation. The ZnO:Sb nanowires possessed a higher absorbance ratio than that of the ZnO nanowires from UV to visible-light range with a redshift effect, which caused a decrease in the bandgap or introduction of intraband gap states, and resulted in more visible-light absorption. Therefore, the photocatalytic activities of ZnO:Sb nanowires were superior to those of the ZnO nanowires.

Acknowledgments

The authors thank the National Science Council of the Republic of China for financially supporting this research under Contract Nos. NSC 97-2221-E-035-004 and NSC 98-2221-E-035-008.

Feng Chia University assisted in meeting the publication costs of this article.

References

1. L. Yang, G. Wang, C. Tang, H. Wang, and L. Zhang, *Chem. Phys. Lett.*, **409**, 337 (2005).
2. C. W. Fang, J. M. Wu, L. T. Lee, Y. H. Hsien, S. C. Lo, and C. H. Chen, *Thin Solid Films*, **517**, 1268 (2008).
3. F. Paraguay, D. M. Miki-Yoshida, J. Morales, J. Solis, and W. Estrada, *Thin Solid Films*, **373**, 137 (2000).
4. C. W. Fang, J. M. Wu, L. T. Lee, H. H. Yeh, W. T. Wu, Y. H. Lin, P. J. Tsai, and Y. R. Chen, *Electrochem. Solid-State Lett.*, **13**, K63 (2010).
5. S. Y. Bae, H. W. Seo, and J. Park, *J. Phys. Chem. B*, **108**, 5206 (2004).
6. J. Zhong, S. Muthukumar, Y. Chen, Y. Lu, H. M. Ng, W. Jiang, and E. L. Garfunkel, *Appl. Phys. Lett.*, **83**, 3401 (2003).
7. H. W. Liang, Y. M. Lu, D. Z. Shen, Y. C. Liu, J. F. Yan, C. X. Shan, B. H. Li, Z. Z. Zhang, J. Y. Zhang, and X. W. Fan, *Phys. Status Solidi A*, **202**, 1060 (2005).
8. C. L. Hsu, S. J. Chang, Y. R. Lin, S. Y. Tsai, and I. C. Chen, *Chem. Commun.*, **2005**, 3571.
9. O. Maksimov and B. Z. Liu, *J. Cryst. Growth*, **310**, 3149 (2008).
10. C. S. Xie, B. L. Zhu, R. Jiang, X. Chen, W. L. Song, J. B. Wang, and J. Shi, *J. Cryst. Growth*, **266**, 511 (2004).
11. A. Weibel, R. Bouchet, S. L. P. Savin, A. V. Chadwick, P. E. Lippens, M. Womes, and P. Knauth, *ChemPhysChem*, **7**, 2377 (2006).
12. T. J. Hsueh, C. L. Hsu, S. J. Chang, Y. R. Lin, S. P. Chang, Y. Z. Chiou, T. S. Lin, and I. C. Chen, *IEEE Trans. Nanotechnol.*, **6**, 595 (2007).
13. T. J. Hsueh, S. J. Chang, C. L. Hsu, Y. R. Lin, I. C. Chen, C. L. Hsu, T. J. Hsueh, and S. P. Chang, *J. Electrochem. Soc.*, **155**, K152 (2008).
14. K. S. Park, Y. J. Choi, M. W. Ahn, D. W. Kim, Y. M. Sung, J. G. Park, and K. J. Choi, *J. Nanosci. Nanotechnol.*, **9**, 4328 (2009).
15. F. X. Xiu, Z. Yang, L. J. Mandalapu, D. T. Zhao, J. L. Liu, and W. P. Beyermann, *Appl. Phys. Lett.*, **87**, 152101 (2005).
16. J. M. Wu, *Thin Solid Films*, **517**, 1289 (2008).
17. J. M. Wu, *J. Phys. Chem. C*, **112**, 13192 (2008).
18. K. Demeestere, J. Dewulf, T. Ohno, P. H. Salgado, and H. V. Langenhove, *Appl. Catal., B*, **61**, 140 (2005).
19. O. Carp, C. L. Huisman, and A. Reller, *Prog. Solid State Chem.*, **32**, 33 (2004).
20. Y. Li, A. Paulsen, I. Yamada, Y. Koide, and J.-J. Delaunay, *Nanotechnology*, **21**, 295502 (2010).
21. Q. Kuang, C. Lao, Z. L. Wang, Z. Xie, and L. Zheng, *J. Am. Chem. Soc.*, **129**, 6070 (2007).
22. S. E. Ahn, J. S. Lee, H. Kim, S. Kim, B. H. Kang, K. H. Kim, and G. T. Kim, *Appl. Phys. Lett.*, **84**, 5022 (2004).